forests

MDPI

Article

Characterization and Functional Analysis of *PmCMK*: A Gene Involved in Terpenoid Synthesis in *Pinus massoniana*

Yiyun Qin, Manqing Peng, Yuan He, Xin He, Zichen Huang, Peihuang Zhu, Qiong Yu and Kongshu Ji *

State Key Laboratory of Tree Genetics and Breeding, Key Laboratory of Forestry Genetics & Biotechnology of Ministry of Education, Co-Innovation Center for Sustainable Forestry in Southern China, Nanjing Forestry University, Nanjing 210037, China; qinyiyun@njfu.edu.cn (Y.Q.); pmq@njfu.edu.cn (M.P.); heyuan@njfu.edu.cn (Y.H.); hexin1234567@njfu.edu.cn (X.H.); huangzichen@njfu.edu.cn (Z.H.); zphzhupeihuang@163.com (P.Z.); yuqiong@njfu.edu.cn (Q.Y.)
* Correspondence: ksji@njfu.edu.cn

Abstract: In *Pinus massoniana*, the methyl-D-erythritol-4-phosphate (MEP) pathway plays a crucial role in the biosynthesis of terpenoids. The fourth step of this pathway is specifically regulated by 4-(cytidine 5′-diphospho)-2-C-methyl-D-erythritol kinase (CMK). In this study, *PmCMK* (MW892445.1) was isolated. As a member of the GHMP kinase family, *PmCMK* exhibits homology with *CMK* genes across diverse species. The examination of relative expression patterns revealed that *PmCMK* exhibited higher expression levels in tissues of *P. massoniana* that are rich in resin. We successfully cloned the *PmCMK* promoter (1654 bp) and integrated it into a GUS reporter vector. This construct was then transformed into the leaves of tobacco (*Nicotiana* × *sanderae*) to assess transient expression patterns. The results demonstrated that the promoter was active not only in the roots, leaves, and stems of the tobacco plants but also exhibited varying expression levels in response to treatments with IAA, SA, MeJA, and PEG6000. This suggested that *PmCMK* expression was modulated by a variety of signals. It revealed that the expression of *PmCMK* was affected by different treatments. Further allogeneic expression studies showed that tobacco overexpressing *PmCMK* exhibited increased levels of chlorophyll and carotene compared to the wild type. This enhancement in content indicates that *PmCMK* has a significant role in isoprene biosynthesis. These findings provide valuable insights for future research aimed at elucidating the biosynthetic pathways of terpenoids and developing breeding strategies to enhance resin production in *P. massoniana*.

Keywords: MEP pathway; CMK; *Pinus massoniana*; terpenoids

check for updates

Citation: Qin, Y.; Peng, M.; He, Y.; He, X.; Huang, Z.; Zhu, P.; Yu, Q.; Ji, K. Characterization and Functional Analysis of *PmCMK*: A Gene Involved in Terpenoid Synthesis in *Pinus massoniana*. *Forests* **2024**, *15*, 1019. https://doi.org/10.3390/f15061019

Academic Editor: Dušan Gömöry

Received: 20 May 2024
Revised: 10 June 2024
Accepted: 11 June 2024
Published: 12 June 2024

Copyright: © 2024 by the authors. Licensee MDPI, Basel, Switzerland. This article is an open access article distributed under the terms and conditions of the Creative Commons Attribution (CC BY) license (https://creativecommons.org/licenses/by/4.0/).

1. Introduction

Terpenoids, a diverse class of compounds produced by plants, encompass important substances such as gibberellins, carotenoids, and chlorophyll. These compounds, also known as isoprene derivatives, are crucial for various aspects of plant growth and development [1,2]. The fundamental structural unit of terpenoids is isoprene (C5H8), and they are classified according to the number of these isoprene units they possess. This classification includes semiterpenes (C5), monoterpenes (C10), sesquiterpenes (C15), diterpenes (C20), triterpenes (C30), and so on [3]. Isoprene in plants is vital for maintaining membrane fluidity, facilitating respiration, and enhancing photosynthesis. In turn, it supports overall plant growth and regulation. These specialized metabolites also play a significant role in mediating the plant's defense and adaptive responses to environmental challenges. They are integral to allelopathic interactions and plant–pathogen relationships, serving to protect plants from herbivores and disease-causing agents, and the volatiles they produce influence the behavior of insects [4]. Additionally, terpenoids are known to attract pollinators and seed-dispersing animals, thereby enhancing the survival and propagation of plant species [5]. The economic significance of isoprenoids extends to various industries, as they serve as crucial components in the production of pharmaceuticals, nutritional supplements,

flavorings, pigments, agrochemicals, and disinfectants, and numerous other applications. This underscores the importance of understanding and harnessing the potential of these bioactive compounds for both ecological and commercial purposes [6].

The biosynthesis of plant terpenoids is a complex process that can be segmented into three principal stages. The initial stage focuses on the synthesis of the fundamental precursors, namely isoprene pyrophosphate (IPP) and dimethylallyl pyrophosphate (DMAPP). The second stage involves the generation of direct precursor compounds, which are then used in the third stage for the synthesis and modification of a diverse array of terpenoid structures [5]. IPP and DMAPP are indispensable precursors in the manufacture of terpenoids, synthesized primarily through two key metabolic pathways. The first metabolic pathway is the mevalonate (MVA) pathway, which operates in the cytoplasm and commences with acetyl-CoA. The second is the 2-C-methyl-D-erythritol-4-phosphate (MEP) pathway, which takes place in the plastids [7]. The MVA pathway is prevalent across diverse organisms, including archaea, certain Gram-positive bacteria, yeast, and animals. Conversely, the MEP pathway serves as the primary route for most Gram-negative bacteria, cyanobacteria, and green algae [8–11]. Many organisms rely solely on one of these pathways, whereas higher plants and specific algae, such as *Cyanidium caldarium* and *Ochromonas danica*, utilize both the MVA and MEP pathways [12–14]. A key enzyme in the MEP pathway is 4-(cytidine 5′-diphospho) -2-C-methyl-D-erythritol kinase (CMK), which catalyzes the transformation of 4-(cytidine 5′-diphospho)-2-C-methyl-D-erythritol (CDE-MP) to 4-(cytidine 5′-diphospho) -2-C-methyl-D-erythritol 2-phosphate (CDE-ME2P) [15,16]. CMK shares significant sequence homology with other kinases, particularly homoserine and mevalvalate kinases. Through studies employing virus-induced gene silencing (VIGS) targeted at the tobacco *CMK* gene, its pivotal role in chloroplast development has been uncovered, resulting in observable reductions in both the number and size of chloroplasts, along with decreased levels of metabolites originating from the MEP pathway, including chlorophyll and carotenoids [17]. In *Ginkgo biloba*, two homologous *CMK* genes, *GbCMK1* and *GbCMK2*, have been successfully cloned and characterized. Their existence suggests a sophisticated regulatory mechanism within the MEP pathway, allowing *G. biloba* to efficiently distribute the precursors IPP and DMAPP between its primary and secondary metabolic processes. This highlights the plant's employment of a multi-faceted regulatory strategy involving CMK isoenzymes to fine-tune its secondary metabolism [18].

P. massoniana belongs to the subgenus of Pinaceae, a family known as the largest within the gymnosperms, characterized by its possession of divascular bundles. This expansive family comprises approximately 10 genera and around 230 species globally, with China alone contributing to approximately 10 genera and roughly 113 species [19]. Members of the Pinaceae family are of paramount importance due to their utility as sources of solid wood and high-quality pulp. Additionally, several species within this family are valuable for the extraction and refinement of various chemical raw materials, such as turpentine. Some species are edible or possess medicinal properties, while others are utilized in ornamental gardening [19,20]. *P. massoniana* particularly stands out for its production of rosin, which is abundant in monoterpenes and diterpenes. This resin is harvested not just for extracting turpentine and rosin but also functions as a biofuel, thereby carrying substantial ecological and economic importance [21]. China accounts for over one-third of the global turpentine production, positioning it as a leading producer. As a result, future research will prioritize understanding the relationship between the components of resin production and pine wood nematodes in the development of high-yielding turpentine varieties [22]. Methyl-D-erythritol-4- phosphate (MEP) pathway serves as a crucial and indispensable metabolic route for terpenoid biosynthesis in *P. massoniana*, with CMK being the sole kinase involved in this pathway [23]. However, despite its significance, there have been no dedicated studies to date exploring the transcriptional expression and regulatory mechanisms of the *CMK* gene in *P. massoniana*. In the present study, we elucidate the function of *PmCMK* through comprehensive analyses, including tissue-specific expression profiling, heterologous expression, and transient transformation,

leveraging the previously identified open reading frame (ORF) and promoter sequences of *PmCMK*. These endeavors are not only instrumental in advancing our understanding of the regulatory pathways governing terpenoid biosynthesis but also contribute significantly to the breeding of high-yielding resin-producing strains of *P. massoniana*.

2. Materials and Methods

2.1. Plant Material

The experimental materials comprised two-year-old potted seedlings of *P. massoniana*, originating from the seed orchard located at the Baisha State-owned Forest Farm in Shanghang, Fujian Province, China. These materials were used to clone the ORF and promoter of *PmCMK*. The samples of *P. massoniana* with high resin production were sourced from Gaolan Village in Xindong Town, Gaozhou City, Guangdong Province, while the samples with low resin production were collected from Zhong Village in Pintai Town, Yunan County, Guangdong Province. They were used to measure the expression of *PmCMK*. For the study, tobacco (*Nicotiana* × *sanderae*) was cultivated in a controlled laboratory setting, with a photoperiod of 16 h of light alternating with 8 h of darkness, maintaining a constant temperature of 24 °C and a light intensity of 100 μmol m^{-2} s^{-1}.

2.2. Cloning of the PmCMK and Bioinformatics Analysis of the Protein Sequence

RNA was extracted from two-year-old potted seedlings of *P. massoniana* using the FastPure Universal Plant TotalRNA Isolation Kit (Nanjing Vazyme Biotech Co., Ltd., Nanjing, China). First-strand cDNA was synthesized using the One-step gDNA Removal and cDNA Synthesis SuperMix kit (Yeasen Biotech, Shanghai, China). The ORF of the *PmCMK* gene (1218 bp) was cloned from the material of *P. massoniana* utilizing the sequence from NCBI (GenBank accession number: MW892445.1). Primers CMK-ORF-F and CMK-ORF-R (Supplementary Table S1) were designed according to the *PmCMK* sequence. A 50 μL PCR system was used. The process involved an initial pre-denaturation step at 98 °C for 1 min, followed by 35 cycles of denaturation at 98 °C for 10 s, annealing at 58 °C for 10 sec and extension at 72 °C for 1 min. Finally, a final extension step was performed at 72 °C for 5 min. After cloning, the pEASY-Blunt vector was connected, transferred into *Escherichia* coli, and the bacterial solution was sent for sequencing (Tsingke Biotechnology Co., Ltd., Beijing, China).

NCBI was used for sequence alignment (https://www.ncbi.nlm.nih.gov/, accessed on 18 March 2024). InterPro (http://www.ebi.ac.uk/interpro/, accessed on 20 March 2024) was used for structure domain analysis. Evolutionary tree was beautified with ITOL (https://itol.embl.de/, accessed on 21 March 2024). Expasy (https://www.expasy.org/, accessed on 1 April 2024) was used to analyze the physicochemical properties of proteins. SignalP4.1 (https://services.healthtech.dtu.dk/services/SignalP-4.1/, accessed on 1 April 2024) was used to analyze the signal peptide. TMHMM Server v. 2.0 (https://services.healthtech.dtu.dk/services/TMHMM-2.0/, accessed on 1 April 2024) was used to analyze the membrane structure domain. The protein secondary structure was analyzed by SOPMA (https://npsa-prabi.ibcp.fr/cgi-bin/npsa_automat.pl?page=npsa_sopma.html, accessed on 3 April 2024). SWISS-MODEL (https://swissmodel.expasy.org/, accessed on 4 April 2024) was used for constructing the model of the protein tertiary structure.

The sequences of high homology to *PmCMK* were obtained by searching the NCBI database with Blastp (Supplementary Table S2). The analysis and prediction of the PmCMK protein was conducted with Jalview 2.11.3.3 software. The phylogenetic tree was constructed utilizing MEGA 5.1 software.

2.3. Relative Expression Levels of PmCMK in High- and Low-Resin-Producing Materials in P. massoniana

The tender shoots of annual seedlings from high-resin-producing and low-resin-producing *P. massoniana* were collected separately. Additionally, seeds from both high- and low-resin-producing *P. massoniana* were cultivated under a photoperiod of 16 h of light

alternating with 8 h of darkness, maintaining a constant temperature of 24 °C and a light intensity of 100 μmol m^{-2} s^{-1} for two months, and the entire plants were then harvested. Expression levels of *PmCMK* were examined in four types of materials: the tender shoots of annual seedlings from high-resin-producing *P. massoniana*, the tender shoots of annual seedlings from low-resin-producing *P. massoniana*, the entire two-month-old plants from high-resin-producing *P. massoniana*, and the entire two-month-old plants from low-resin-producing *P. massoniana*. The four materials are shown in Supplementary Figure S1. We employed the FastPure Universal Plant TotalRNA Isolation Kit (Nanjing Vazyme Biotech Co., Ltd.) to extract RNA from the samples in high- and low-resin-producing materials.

The differential expression of the *PmCMK* gene across various tissues was examined through reverse transcription quantitative polymerase chain reaction (RT-qPCR). RT-qPCR was performed using the SYBR Green method. The 10 μL reaction mixture consisted of 1 μL of 20-fold diluted cDNA, 5 μL of SYBR Green Real-time PCR Master Mix, 0.4 μL each of 10 μM primers, and 3.2 μL of ddH_2O. The composition of the reaction system and the amplification protocol adhered to the instructions in the Hieff UNICON Universal Blue qPCR SYBR Green Master Mix manual. The relative transcript abundance was determined using the $2^{-\Delta\Delta Ct}$ method. Each qRT-PCR result was conducted with three biological replicates and three technical replicates. Biological replicates were three *P. massoniana* samples from different single plants with the same growth conditions and the same parts. The three technical replicates were experimental replicates. Data were organized and analyzed using Excel 2021, and graphs were plotted in GraphPad Prism 8.0.2.

2.4. Promoter Cloning and Transient Expression Analysis

DNA was extracted from *P. massoniana* using the FastPure Plant DNA Isolation Mini Kit-BOX2 (Nanjing Vazyme Biotech Co., Ltd.). Based on the sequence of the *PmCMK* promoter (1654 bp), a set of primers was designed for amplification, utilizing the genomic DNA (gDNA) of *P. massoniana* as the template. To predict the cis-acting elements within the cloned promoter sequences, the PlantCARE database was utilized. Primers, incorporating restriction sites for HindIII and BamHI, were designed based on the pBI121 vector, which contains GUS tags and the promoter sequence. Transient expression vectors, pBI121-PmCMK pro::GUS, were constructed and subsequently transformed into *Agrobacterium* GV3101 cells, along with the empty plasmid vector pBI121-CaMV::GUS as a control. After that, the leaves of a 20-day-old tissue culture of tobacco seedlings under aseptic conditions were transformed using the *Agrobacterium*-mediated method [5]. After the transformation, the plants underwent a 2-day dark treatment at 28 °C. Subsequently, the leaves of different groups were sprayed with 100 μM indole-3-acetic acid (IAA), 100 μM salicylic acid (SA), 100 μM methyl jasmonate (MeJA), and 20% polyethylene glycol 6000 (PEG6000). Each experiment involved three biological replicates and three technical replicates. The leaves were then stained with GUS dye, incubated overnight at 37 °C, and decolorized using 75% ethanol to remove chlorophyll. Finally, the GUS staining was visualized under a stereo-fluorescence microscope (M205FA, Leica, Wetzlar, Germany) for photographic documentation. This process allowed for a qualitative assessment of GUS expression in response to various treatments, providing valuable insights into the regulatory mechanisms of the *PmCMK* promoter.

2.5. Genetically Modified Tobacco

In this experiment, an *Agrobacterium*-mediated transformation method was employed for the infection of wild safflower tobacco. Initially, *Agrobacterium* was cultured in 1 mL of Luria–Bertani (LB) medium and incubated with shaking at 28 °C for one day. The bacterial culture was then transferred to 5 mL of fresh LB medium supplemented with 50 mg/mL kanamycin (Kan) and incubated overnight with shaking at 28 °C. The following day, 1 mL of the overnight bacterial culture was aseptically transferred to 50 mL of LB medium containing 50 mg/mL Kan and 25 mg/mL rifampicin (Rif), and the culture was shaken at 28 °C until the optical density at 600 nm (OD_{600}) reached a range of 0.4 to 0.6. The infiltration

solution was prepared by ddH_2O containing 10 mM $MgCl_2$, 10 mM MES, and 200 μM AS, and the ratio of the infiltration solution used to resuspend the bacterial suspension to the original volume of the bacterial suspension was 1:1. Leaves from two-month-old tobacco plants were trimmed into 1 × 1 cm pieces and immersed in the infection solution, shaking gently for approximately 10 min. The inoculation method referred to the method used by Heidari [24]. Afterward, the infection solution was decanted, and the leaves were blotted dry before being placed on Murashige and Skoog (MS) medium containing 2.0 mg/L 6-benzylaminopurine (6-BA) and 0.5 mg/L IAA to facilitate the infection process. The plants were then subjected to two days of dark incubation followed by a photoperiod of 16 h of light and 8 h of darkness with a constant temperature of 24 °C and a light intensity of 125 μmol m^{-2} s^{-1}. Five days post-infection, the tobacco leaves were transferred to an MS medium containing 2.0 mg/L 6-BA, 0.5 mg/L IAA, 500 mg/L cefotaxime (Cef), and 50 mg/L Kan to select for transformed cells. Under the same conditions as the previous stage, approximately 30 days later, small green regenerated shoots began to emerge around the inoculated leaves. These shoots were excised and cultured in a root induction medium (1/2 MS supplemented with 25 mg/L Kan and 100 mg/L Cef) to encourage root development. Once the tissue culture seedlings had developed a robust root system, they were transplanted into soil to continue their growth and development. The tobacco seedlings were genetically analyzed at the DNA level to confirm the presence of the transgene and to quantify the number of successfully transformed seedlings. This process ensured the successful generation of transgenic tobacco plants for further study and application.

2.6. The Contents of Chlorophyll a, Chlorophyll b, Carotenoid, and CMK

Fresh transgenic tobacco leaves were selected as the sample. The contents of chlorophyll a, chlorophyll b, and carotenoid were determined by the reagents in the plant chloroplast pigments' (chlorophyll a, b, and carotenoids) detection kit (Shanghai Hengyuan Biotechnology Co., Ltd., Shanghai, China). CMK activity in transgenic tobacco was determined by the plant CMK ELISA kit (Shanghai Hengyuan Biotechnology Co., Ltd.).

2.7. Relative Expression Levels of Genes Related to Terpenoid Synthesis Pathways in Transgenic Tobacco

The relative expression levels of genes associated with the terpenoid synthesis pathway were determined using the RT-qPCR method. The selected tobacco genes were as follows: *DXS* and *DXR* from the MEP pathway, *HMGR* and *MK* from the MVA pathway, *GGPPS* from the GGPP pathway, *PSY* and *ZDS* from the lycopene pathway, *β-LCY* prior to the downstream β-carotene generation, and *BCH2* from the zeaxanthin pathway. The primer sequences are provided in Supplementary Table S1. The gene name and GenBank ID of genes related to the terpene synthesis pathway are provided in Supplementary Table S3. The methodology and reaction system employed for RT-qPCR were identical to those described in Section 2.3.

2.8. Statistical Analysis

Each experimental result was derived from three biological replicates and three technical replicates. Data were organized and calculated using Excel, and GraphPad Prism 8.0.2 was utilized for plotting. * represents the *p*-value of the statistical test, where * indicates $p < 0.05$, ** indicates $p < 0.01$, *** indicates $p < 0.001$, and **** indicates $p < 0.0001$.

3. Results

3.1. Cloning of the PmCMK and Bioinformatics Analysis of the Protein Sequence

The ORF of the *PmCMK* gene was cloned (Figure 1A). This ORF encoded 405 amino acids, possessing a theoretical isoelectric point (pI) of 6.71 and a calculated molecular weight of 44.34 kDa. The protein had a total of 41 negatively charged residues (Asp + Glu) and 40 positively charged residues (Arg + Lys), with their respective numbers and proportions presented in Figure 1B. The instability coefficient (II) was 37.46 as a stable protein. The total

average hydrophilic index (GRAVY) was −0.303, its lipid solubility index was 73.01, so the protein was a hydrophilic protein (Figure 1C). It contained no signal peptide and was a non-secreted protein (Figure 1D). The prediction of the transmembrane region indicated that the protein did not have a transmembrane helical region, and all amino acids at positions 1−405 were located on the membrane surface (Figure 1E). The analysis and prediction of the protein's secondary structure revealed that it was primarily composed of 175 uncoiled structures, accounting for 43.21%, followed by 148 α-helices, accounting for 36.54% (Figure 1F). Figure 1G presents the predicted three-dimensional structure pattern.

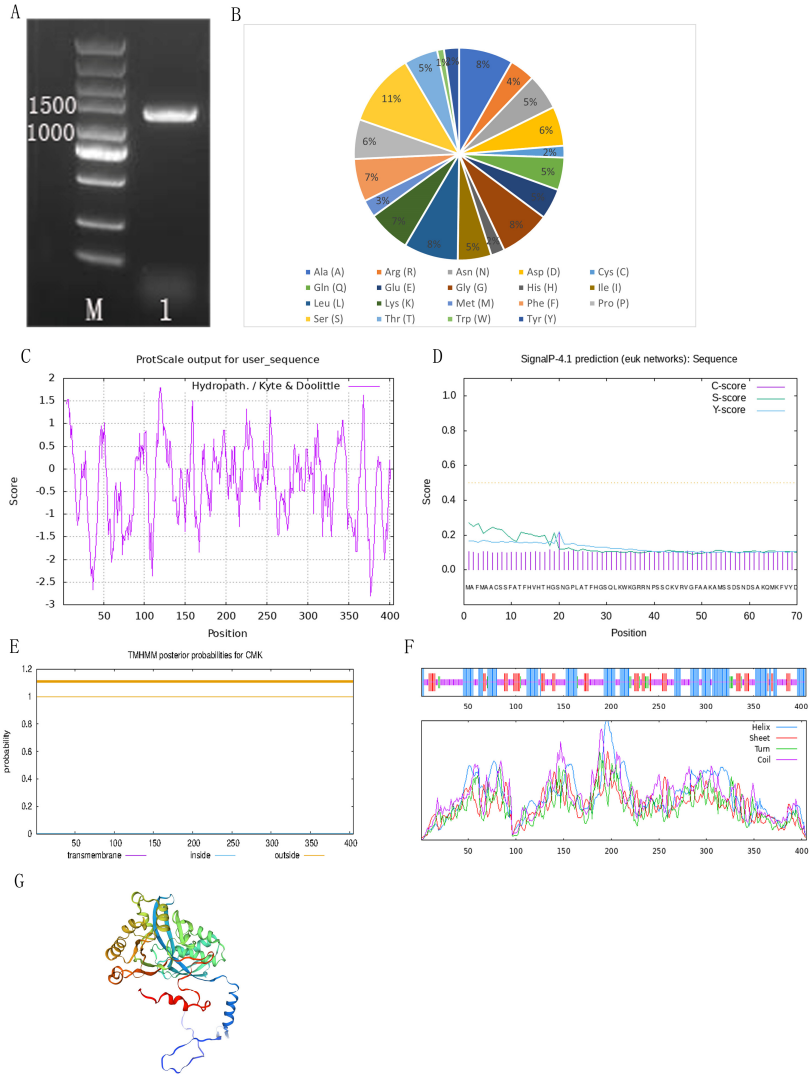

Figure 1. Cloning and sequence analysis of PmCMK protein. (**A**) Cloning of the ORF of *PmCMK* (PCR amplification product of the ORF fragment). (**B**) Number and proportion of their amino acids. (**C**) Hydrophilicity of PmCMK protein. (**D**) Prediction of PmCMK signal peptide. (**E**) Prediction of PmCMK transmembrane domain. (**F**) Prediction of the protein secondary structure of PmCMK. (**G**) Prediction of the three-dimensional structure pattern.

The analysis and prediction of the PmCMK protein revealed the presence of a GHMP kinase N-terminal domain (highlighted with a solid red box) and a GHMP kinase C-terminal domain (highlighted with a solid green box), indicating that *PmCMK* belongs to the GHMP kinase family (Figure 2A and Supplementary Table S2). A phylogenetic tree was constructed to illustrate the evolutionary relationship between the *PmCMK* gene and *CMK* genes in other plants, taking into account the protein sequence of PmCMK alongside CMK protein sequences from diverse species. It can be seen that all of these

proteins have the GHMP kinase domain and that PmCMK is more closely related to the CMK of gymnosperms such as *P. kesiya*, *G. biloba*, and *Cryptomeria japonica* (Figure 2B and Supplementary Table S2).

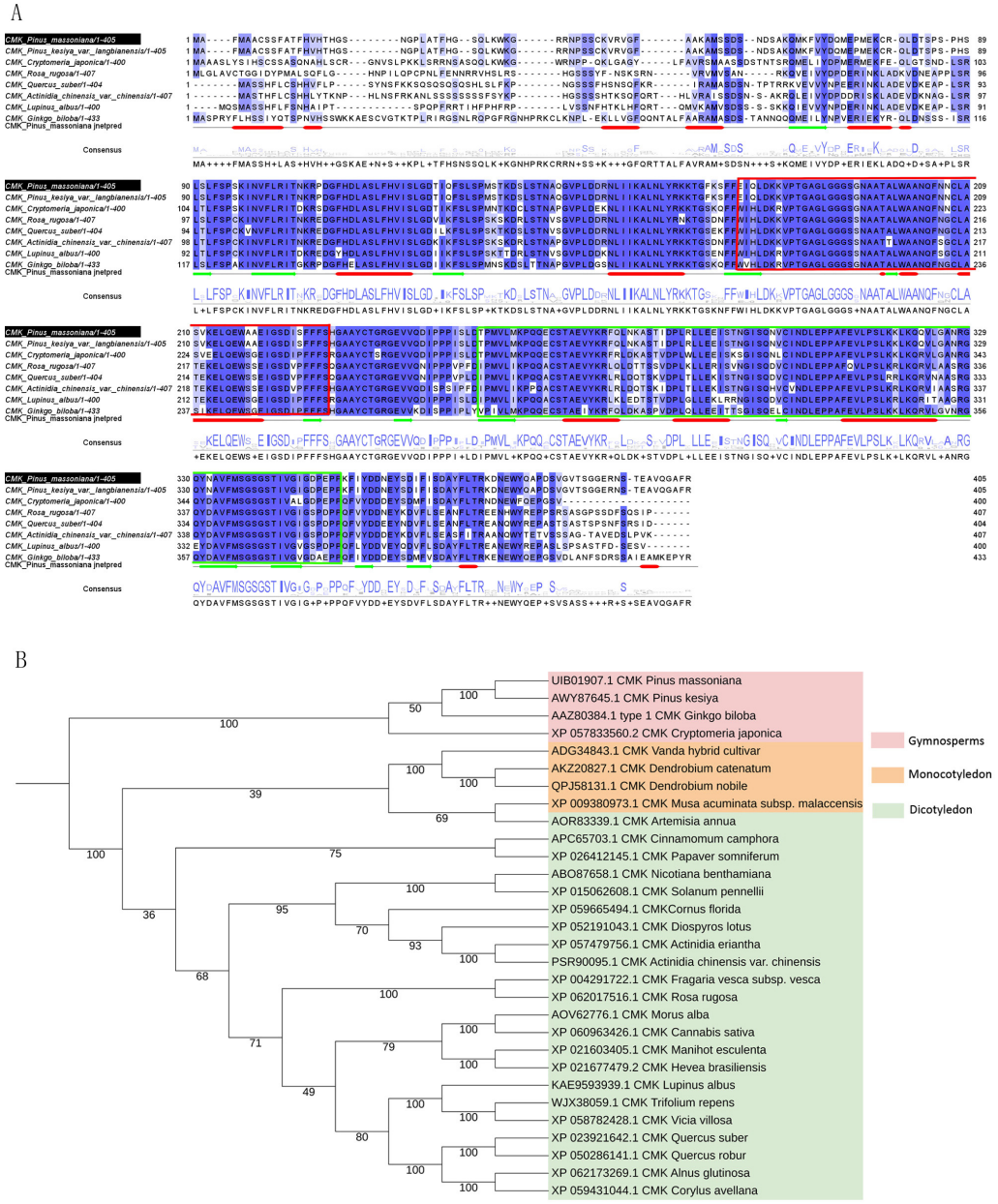

Figure 2. Amino acid sequence analysis and phylogenetic analysis of *PmCMK*. (**A**) Amino acid comparison of *PmCMK* in *Pinus massoniana* with homologous genes of other species. (**B**) Phylogenetic relationship between *PmCMK* and *CMK* genes in other plants. Notes: In (**A**), the red box marks the GHMP kinase N terminal domain, the green box marks the GHMP kinase C terminal domain; In (**B**), gymnosperms are light red, monocotyledons are orange, and dicotyledons are light green.

3.2. Relative Expression Levels of PmCMK in High- and Low-Resin-Producing Materials in P. massoniana

As shown in Figure 3, both in the shoots and the entire materials of *P. massoniana*, the expression of *PmCMK* was more prominent in high-resin seedlings compared to low-resin seedlings. This finding points to a potential significant role of *PmCMK* in resin production in *P. massoniana*, with its expression being correlated with the resin content of the seedlings.

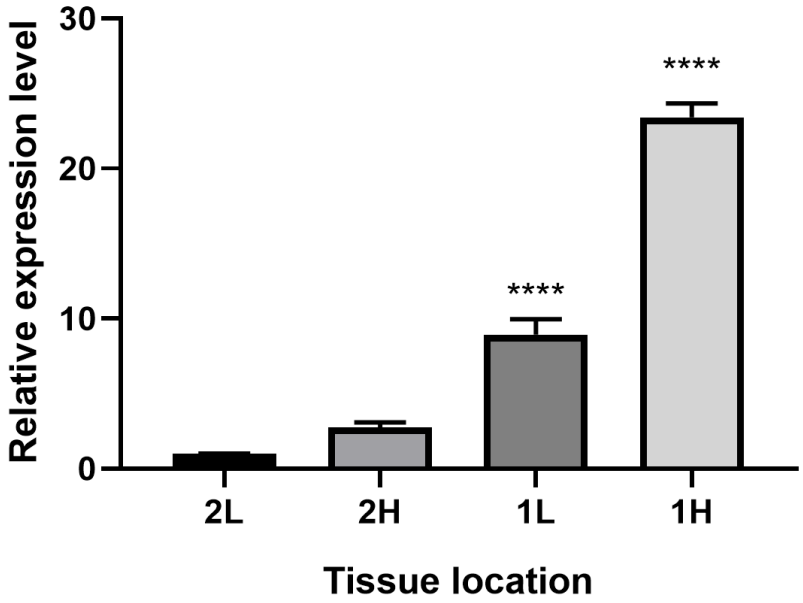

Figure 3. Expression of *PmCMK* gene in high/low-resin producing seedlings of *P. massoniana.* Notes: H represented high-resin seedlings materials, L represented low-resin seedlings materials, 1 represented one-year-old trees, 2 represented materials with a growth duration of two months, $p < 0.0001$ is represented by ****.

3.3. Function Analysis of PmCMK Promoter

The prediction results of the cis-acting elements of the *PmCMK* promoter indicated that the promoter sequence encompassed a variety of cis-acting elements (Figure 4 and Supplementary Table S4). The *PmCMK* promoter contained not only common eukaryotic elements such as the CAAT-box and TATA-box, which are fundamental to the initiation of transcription, but also photoresponse elements like the ATCT-motif and MRE, as well as the TCCC-motif. Moreover, the promoter sequence harbored elements associated with responses to MeJA (CGTCA-motif), salicylic acid (TCA-element), and growth hormones (TGA-element), suggesting its potential role in hormone signaling pathways. Additionally, the *PmCMK* promoter was enriched with stress-responsive elements, such as those involved in drought induction (MBS) and anaerobic induction (ARE), highlighting its possible role in mediating stress responses in *P. massoniana*. This comprehensive analysis of the *PmCMK* promoter provides valuable insights into its regulatory mechanisms and its potential as a tool for manipulating gene expression in response to various environmental cues.

The experimental findings indicated that in the negative control group, none of the tobacco tissues exhibited staining, whereas all tissues from the positive control and experimental groups displayed a blue coloration (Figure 5A). Specifically, the wild tobacco tissues infected with the positive control showed a distinct blue, indicative of robust promoter activity. It is noteworthy that β-glucuronidase (GUS) expression was observed even in the absence of an inducer, indicating that the promoter regions can drive gene expression without external stimulation. These results provide valuable insights into the regulatory mechanisms of the *PmCMK* promoter and its potential applications in plant biotechnology.

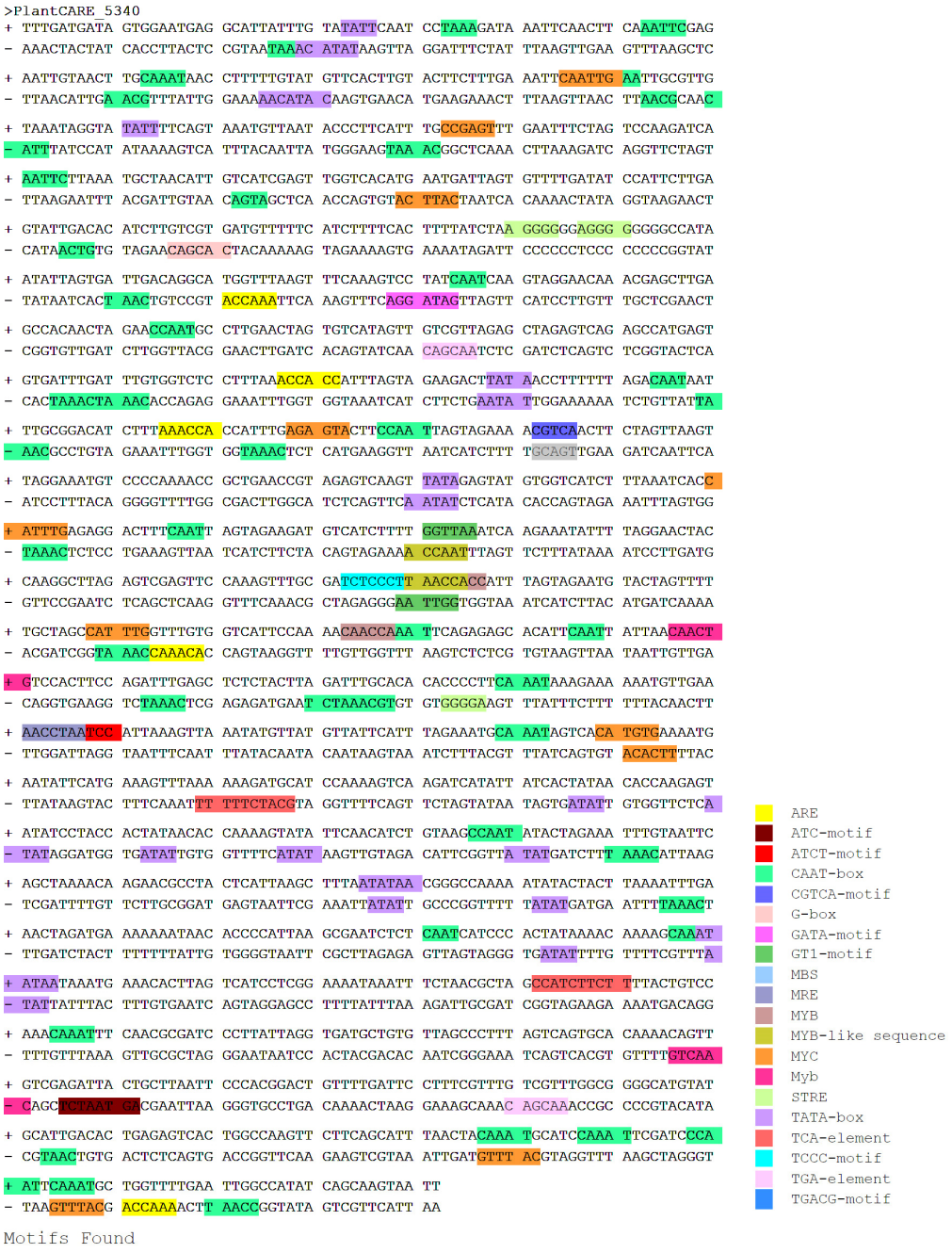

Figure 4. Analysis of cis-acting elements of the *PmCMK* promoter.

Based on the predictions of cis-acting elements within the promoter, four reagents were selected for treating tobacco leaves, IAA, SA, MeJA, and PEG6000, which were applied on the second day post-infection. As depicted in Figure 5B, the *PmCMK* promoter sequences exhibited variable responses to the different hormonal treatments and drought stress simulation. When compared to the untreated control group, the expression levels of the *PmCMK* promoter were notably enhanced in response to MeJA and IAA treatments. This observation suggests that the *PmCMK* promoter is susceptible to regulation by both MeJA and IAA hormones, which in turn can modulate the expression of the *PmCMK* gene. These findings underscore the potential of the *PmCMK* promoter as a target for hormonal regulation in plant metabolic engineering and biotechnology applications.

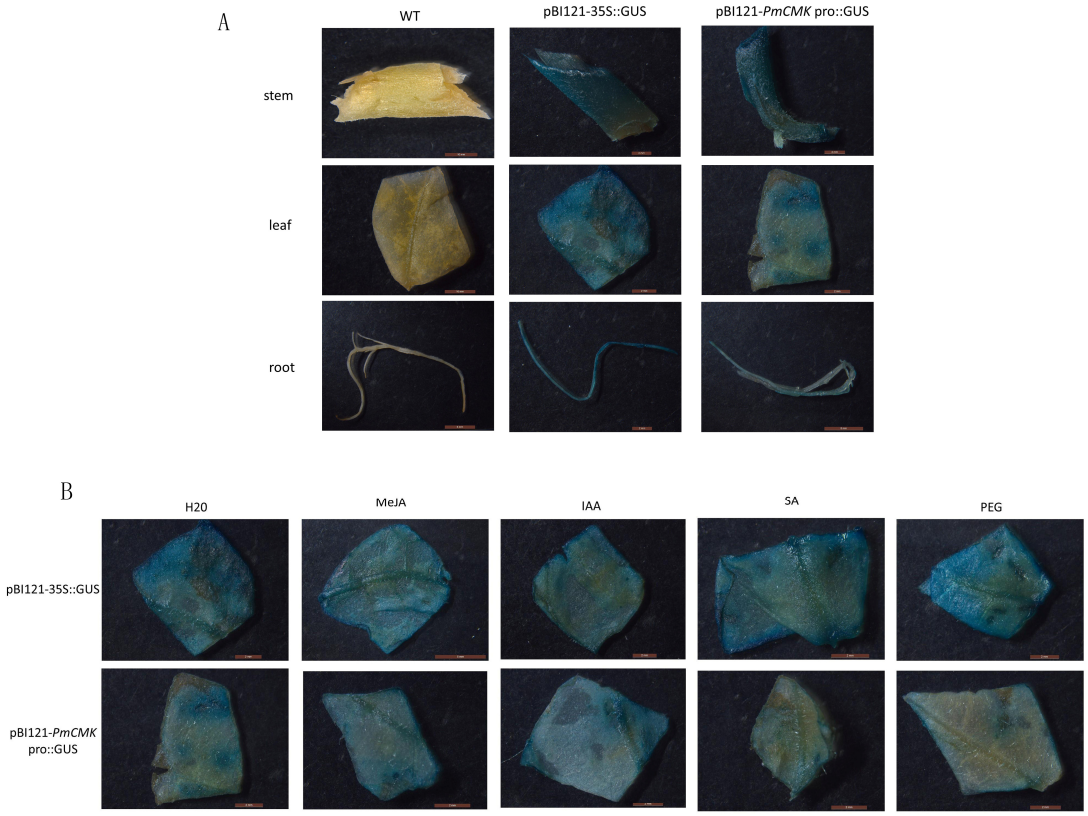

Figure 5. Transient expression of the *PmCMK* promoter. (**A**) Activity in various tissues of tobacco with transient transfer of the *PmCMK* promoter. (**B**) Response of *PmCMK* promoter under four treatments.

3.4. Overexpression of PmCMK in Tobacco Promotes the Content of Carotenoids

Transgenic plants were detected at the DNA level (Figure 6A). The result showed that the expression levels of different overexpression lines (OE) were different (Figure 6B). Among the eight tested OE lines, OE9 exhibited the highest expression level. Three OE lines with high expression, specifically OE9, OE25, and OE28, were selected for phenotypic observations, followed by assessments of their respective pigment and enzyme contents. The phenotype of transgenic tobacco with the highest relative expression of *PmCMK* was not obvious during vegetative growth (Supplementary Figure S2).

The CMK activity of wild-type and transgenic tobacco was detected. As depicted, the CMK activity of transgenic tobacco was significantly higher than that of wild-type tobacco, and the enzyme activity of OE28 was the highest, attaining 1.23 times the level of the wild type, while the CMK enzyme activity in OE9 and OE25 was approximately 1.16 times that of the wild type. These results indicate that the introduction of the *PmCMK* gene into tobacco leads to an enhancement in CMK activity (Figure 7A).

The comparison of photosynthetic pigment content between wild-type tobacco and the one overexpressing *PmCMK* showed that chlorophyll a (Figure 7B), chlorophyll b (Figure 7C), and carotenoid (Figure 7D) were enhanced compared with the wild type. Chlorophyll a was found to be 3.38, 2.25, and 2.69 times higher than that of the wild type, respectively. Among the transgenic lines, OE9 exhibited the highest chlorophyll a content, reaching 0.5836 mg/g, while OE25 had the lowest, at 0.3881 mg/g. Chlorophyll b levels were elevated by 2.85, 1.89, and 2.29 times compared to the wild type, with OE9 showing the highest expression at 7.5490 mg/g, and OE25 having the lowest carotenoid content at 5.0090 mg/g. In the case of carotenoids, increases of 4.50, 1.69, and 2.18 times were observed. OE9 possessed the highest carotenoid content, reaching 0.7929 mg/g, while OE25 had the lowest at 0.2972 mg/g.

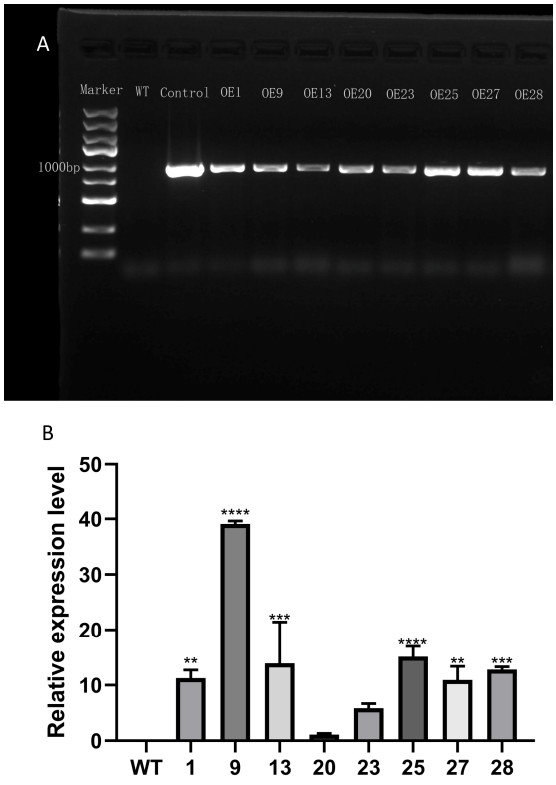

Figure 6. Validation, expression, and phenotype of transgenic tobacco. (**A**) Validation of genetically modified tobacco. (**B**) Relative expression of *PmCMK* in different overexpression lines. Note: "*" indicates that there is a difference compared with the "WT" group; ** $p < 0.01$, *** $p < 0.001$, **** $p < 0.0001$.

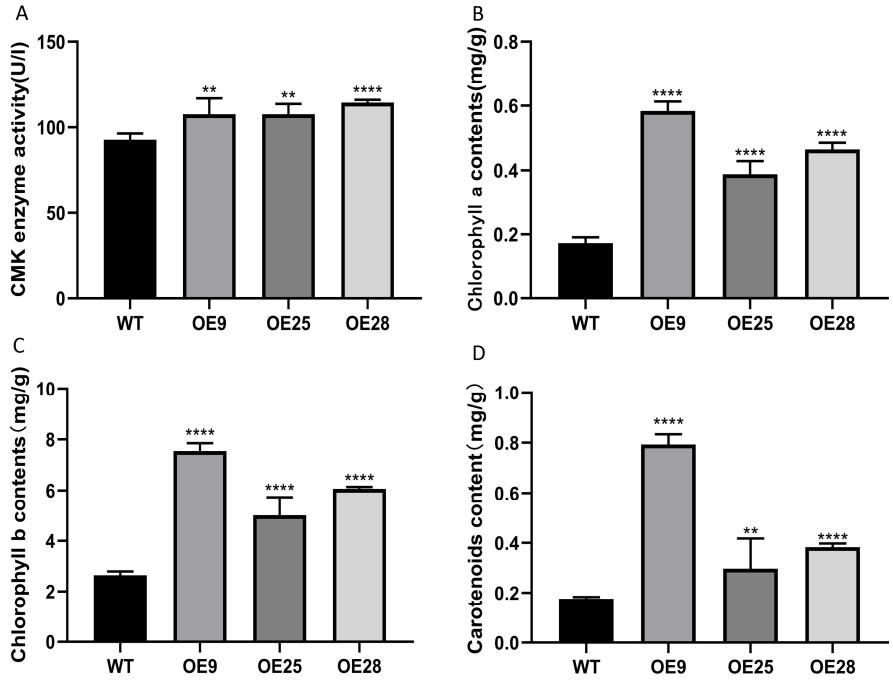

Figure 7. Contents of pigment and enzyme in the tobacco overexpressing *PmCMK* and the wild type (WT). (**A**) 4-(cytidine 5′-diphospho)-2-C-methyl-D-erythritol kinase (CMK) activity. (**B**) Contents of chlorophyll a. (**C**) Contents of chlorophyll b. (**D**) Contents of carotenoids. Note: "*" indicates that there is a difference compared with the "WT" group; ** $p < 0.01$, **** $p < 0.0001$.

3.5. Overexpression of PmCMK in Tobacco Partly Promotes the Content of Genes Related to Terpenoid Synthesis

The result was used to analyze the expression levels of various genes related to the terpenoid synthesis pathway (Figure 8). The selected tobacco genes were as follows: *NtDXS* and *NtDXR* in the MEP pathway, *NtHMGR* and *NtMK* in the MVA pathway, *NtGGPPS* in the GGPP pathway, *NtPSY* and *NtZDS* in the lycopene pathway, *Ntβ-LCY* before the downstream β-carotene generation, and *NtBCH2* in the zeaxanthin pathway. Wild-type tobacco lines were used as the negative control group in the experiment, and the reference gene was *NtActin7* (Gene ID: 107831145) of tobacco. We found that *NtDXS*, *NtDXR*, *NtHMGR*, *NtPSY*, *NtPDS*, *NtZDS*, *Ntβ-LCY*, and *NtBCH2* increased in gene expression, while *NtGGPPS*, *NtMK*, and *NtTPS* decreased in gene expression. This suggested that the overexpression of *PmCMK* in tobacco partly enhances the expression of some terpene synthesis pathway-related genes in tobacco. At the same time, there was also a decrease in the expression levels related to terpene synthesis, suggesting that *PmCMK*'s influence on terpene synthesis pathways is a relatively complex physiological process.

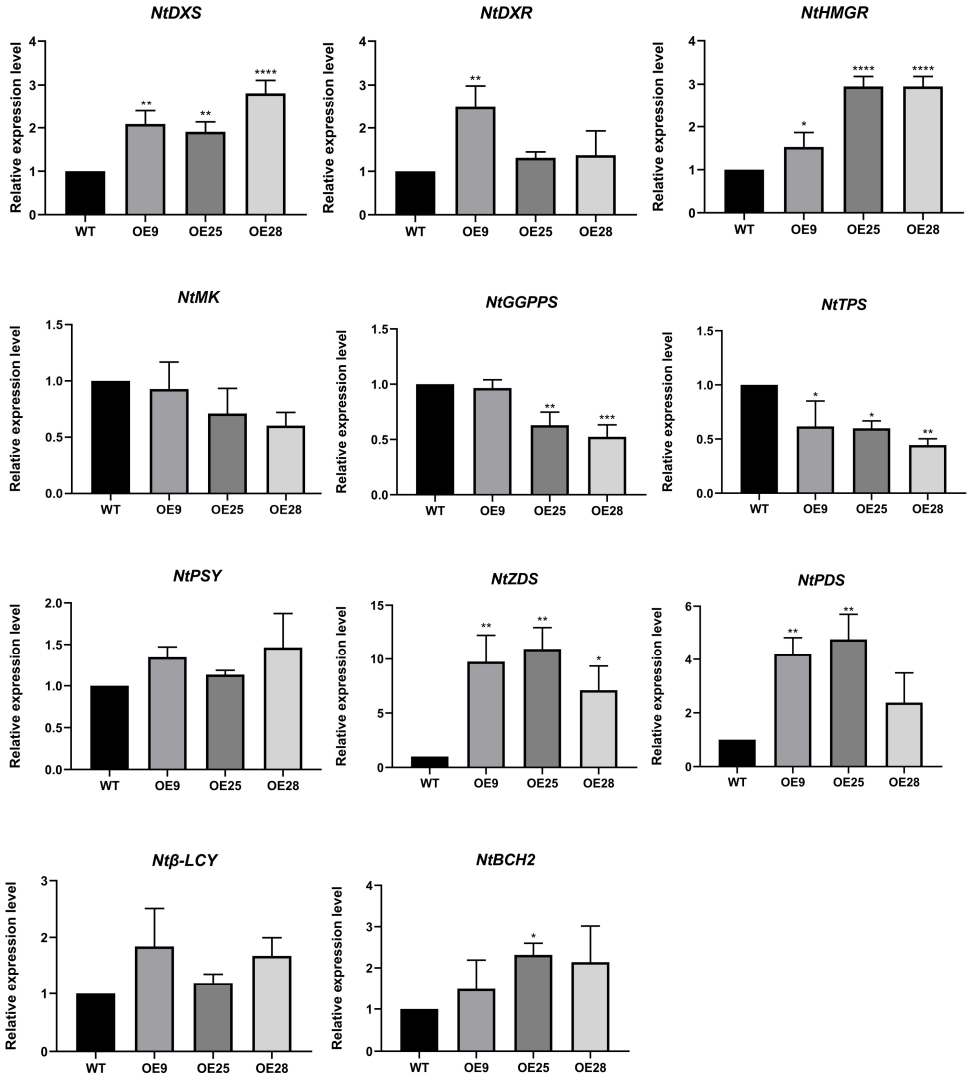

Figure 8. Relative expression level of genes related to the terpenoid synthesis pathway in tobacco overexpressing *PmCMK*. Note: "*" indicates that there is a difference compared with the "WT" group; * $p < 0.05$, ** $p < 0.01$, *** $p < 0.001$, **** $p < 0.0001$.

4. Discussion

Terpenoids constitute a class of natural compounds that are abundantly found in higher plants, primarily derived from isoprene (C5H8). Terpenoids generated by plants, such as gibberellins, carotenoids, and chlorophyll, play important roles in plant growth and development [2]. The metabolites derived from terpenoid compounds can specifically function in mediating interactions between tissues or defense and adaptive responses pertaining to the environment [25]. The MEP pathway, as a crucial metabolic route for the synthesis of terpenoids in plants, represents a significant component in terpenoid research. This article focused on the *PmCMK* gene, which has yet to be investigated in *P. massoniana*, aiming to clone and elucidate its function, thereby contributing novel insights to the study of the MEP pathway in *P. massoniana*. In this paper, *PmCMK* gene was cloned, and a bioinformatics analysis was performed. The results of the conserved domain analysis showed that *PmCMK* had the GHMP kinase domain of the GHMP family. This family comprises unique ATP-dependent enzymes, wherein GHMP kinases feature a conserved Gly/Ser-rich region that plays a crucial role in ATP binding, isoprenoid and amino acid biosynthesis, as well as carbohydrate metabolism [26–28]. In this paper, materials with a high and low resin production were collected, and the relative expression levels were measured. The results indicated that in both the shoots and the entire plants, the expression of *PmCMK* was notably more pronounced in high-resin seedlings as compared to their low-resin counterparts (Figure 3), which also verified the important role of *PmCMK* in the resin production pathway of *P. massoniana*. Previous identification results have established a positive correlation between the expression level of the *PmGGPPS* gene and resin production, with the expression of *PmGGPPS* largely aligning with the varying trends in resin production, both high and low [29]. This provides a certain reference for further research on the expression of terpene-related genes in high- and low-resin-producing *P. massoniana* seedlings in the future.

A correlation between MeJA and terpene metabolism has been established in numerous studies [30,31]. MeJA treatment increases the production of monoterpenes and diterpenes of wood in *Picea abies*, along with a corresponding increase in the activities of their respective terpenoid synthases, indicating that MeJA can enhance the transcription of genes responsible for resin acid biosynthesis [32,33]. Previous studies have demonstrated hormonal effects on terpene production and *TPS* gene expression, with MeJA serving as a crucial component of terpenes that play a vital role in defense mechanisms in kiwifruit (*Actinidia chinensis* Planch.). An exogenous application of SA to kiwifruit produced significant damage on the surface of kiwifruit berries, whereas no notable phenotypic changes were observed after MeJA treatment. Interestingly, when kiwifruit berries were treated with a combination of MeJA and SA, the SA-induced damage on the fruit surface was significantly reduced, indicating that MeJA is effective in mitigating SA-induced damage [34]. Moreover, previous research has revealed disparities in the expression of *PmCMK* in *P. massoniana* under SA and MeJA treatments, which is consistent with the identification of cis-acting elements within the *PmCMK* promoter presented in this paper [28].

In this study, the content of CMK, chlorophyll, and carotenoid in the overexpression lines was observed to be higher than in the wild type, suggesting that the overexpression of *PmCMK* affects the synthesis of these terpenoids. Furthermore, we discovered an upsurge in the expression levels of *DXS* and *DXR* in the MEP pathway of the transgenic tobacco. Based on previous research on *DXS* and *DXR* in the terpenoid synthesis pathway, DXS stands out as a highly regulated enzyme, acting as a crucial rate-limiting step in the MEP pathway across various plant species, and is an effective target for regulating the synthesis of terpenoids in plants [35,36]. *PmCMK* increased the expression levels of *DXS* and *DXR*, which greatly affected the rate of the MEP pathway, and thus affected the synthesis and regulation of terpenoids. In transgenic plants, the expression of *HMGR* in MVA pathway also increases, while the expression of *MK* decreases, indicating that genes in the MEP pathway have a certain impact on genes in the MVA pathway. Furthermore, the expression levels of *PSY*, *ZDS*, *β-LCY* of the β-carotene pathway and *BCH2* of the zeaxanthin pathway

in transgenic lines were higher than those of the wild type. This suggests that *PmCMK* genes have a greater influence on the downstream terpenoid processing pathways, and that the increase in the expression of these genes also corresponds to the increase in the expression of chlorophyll and carotene in the previous transgenic tobacco. This indicates that *PmCMK* affects the production of terpenoids to a certain degree, and this effect is complex, as various genes exert different effects during distinct stages of the terpenoid synthesis pathway. This is consistent with the results shown in the study of the tomato fruit's MEP pathway, where *SlWRKY35* activation positively regulated carotenoid biosynthesis. In that study, they found that *SlWRKY35* overexpression could increase the expression of most genes in the carotenoid synthesis pathway. However, compared to the downstream pathway, the expression of genes in the upstream carotenoid synthesis pathway was notably higher. The overexpression of *SlWRKY35* had a more profound effect on the expression of MEP pathway genes, particularly *DXS1* in tomatoes. This underscores the complexity of the terpenoid synthesis pathway [37].

5. Conclusions

In this study, both the ORF and the promoter of *PmCMK* were cloned, and we performed an expression analysis. Our results revealed that *P. massoniana* with higher resin yields exhibited significantly higher expression levels of *PmCMK*, suggesting a strong correlation between *PmCMK* expression and terpenoid synthesis. Stable transformation experiments in tobacco demonstrated that the overexpression of *PmCMK* led to an increase in the levels of CMK in transgenic tobacco, along with elevations in the concentrations of chlorophyll a, chlorophyll b, and carotenoids. This indicates that enhancing *PmCMK* expression can bolster the production of metabolites along the terpenoid biosynthetic pathway. Furthermore, partial genes associated with terpene biosynthesis were found to be upregulated in the transgenic tobacco, suggesting that *PmCMK* plays a pivotal role in the anabolic processes of terpenes. At the same time, the downregulation of the expression levels of certain terpene-related genes indicates that *PmCMK*'s influence on terpene-related synthesis is a complex process. The analysis of the *PmCMK* promoter and transient transformation assays in tobacco revealed that the *PmCMK* promoter harbors a variety of cis-acting elements that are responsive to external hormonal cues. In summary, this study offers valuable insights into the role of *PmCMK* in the terpene biosynthesis pathway in *P. massoniana*, emphasizing its potential as a key regulatory factor in the production of rosin and other terpenoid compounds.

Supplementary Materials: The following supporting information can be downloaded at: https://www.mdpi.com/article/10.3390/f15061019/s1, Figure S1: High- and low-resin material of *P. massoniana*. Figure S2: Phenotype of transgenic tobacco. Table S1: Primer sequences used in this study. Table S2: The plant name and GenBank ID involved in amino acid sequence analysis and phylogenetic analysis. Table S3: Gene name and GenBank ID of genes related to the terpene synthesis pathway in tobacco. Table S4. Part of the functional prediction of the *PmCMK* promoter cis-acting element.

Author Contributions: Conceptualization, Y.Q.; data curation, Y.Q.; formal analysis, Y.Q.; funding acquisition, K.J.; investigation, Y.Q.; methodology, K.J., Y.Q., M.P., X.H. and Y.H.; software, Y.Q. and Y.H.; validation, Y.Q. and Z.H.; visualization, Y.Q. and Y.H.; writing—original draft, Y.Q.; writing—review and editing, K.J., Q.Y. and P.Z. All authors have read and agreed to the published version of the manuscript.

Funding: The research was financially supported by the National Key R&D Program of China (2022YFD2200202) and the Priority Academic Program Development of Jiangsu Higher Education Institutions (PAPD).

Data Availability Statement: Data is contained within the article or Supplementary Material.

Acknowledgments: We thank Yanling Cai (Guangdong Academy of Forestry, Guangdong Province, China) for providing high-resin and low-resin *P. massoniana* seeds; We also thank Jingquan Lin and Nengqing Lin (senior engineers at Baisha State-owned Forest Farm in Shanghang, Fujian Province, China) for providing seeds from the *P. massoniana* seed orchard.

Conflicts of Interest: The authors declare no conflicts of interest.

References

1. Pallardy, S.G. Plant hormones and other signaling molecules. In *Physiology of Woody Plants*, 3rd ed.; Academic Press: Cambridge, MA, USA, 2008; pp. 367–377.
2. Tripathy, B.C.; Pattanayak, G.K. Chlorophyll biosynthesis in higher plants. In *Photosynthesis: Plastid Biology, Energy Conversion and Carbon Assimilation*; Springer: Dordrecht, The Netherlands, 2012; pp. 63–94.
3. Chen, J.; Zhao, D.G. Research progress on enzymes related to plant terpenoid biosynthesis and their coding genes. *Mol. Plant Breed.* **2004**, *6*, 757–764.
4. Yactayo-Chang, J.P.; Broadhead, G.T.; Housler, R.J.; Resende, M.F.R.; Verma, K.; Louis, J. Maize terpene synthase 1 impacts insect behavior via the production of monoterpene volatiles β-myrcene and linalool. *Phytochemistry* **2024**, *218*, 113957. [CrossRef] [PubMed]
5. Tholl, D. Biosynthesis and biological functions of terpenoids in plants. In *Biotechnology of Isoprenoids*; Springer: Cham, Switzerland, 2015; pp. 63–106.
6. Vranová, E.; Coman, D.; Gruissem, W. Network analysis of the MVA and MEP pathways for isoprenoid synthesis. *Annu. Rev. Plant Biol.* **2013**, *64*, 665–700. [CrossRef] [PubMed]
7. McGarvey, D.J.; Croteau, R. Terpenoid metabolism. *Plant Cell* **1995**, *7*, 1015. [PubMed]
8. Smit, A.; Mushegian, A. Biosynthesis of isoprenoids via mevalonate in *Archaea*: The lost pathway. *Genome Res.* **2000**, *10*, 1468–1484. [CrossRef] [PubMed]
9. Welsch, R.; Maass, D.; Voegel, T.; DellaPenna, D.; Beyer, P. Transcription factor RAP2.2 and its interacting partner SINAT2: Stable elements in the carotenogenesis of Arabidopsis leaves. *Plant Physiol.* **2007**, *145*, 1073–1085. [CrossRef]
10. Disch, A.; Rohmer, M. On the absence of the glyceraldehyde 3-phosphate/pyruvate pathway for isoprenoid biosynthesis in fungi and yeasts. *FEMS Microbiol. Lett.* **1998**, *168*, 201–208. [CrossRef] [PubMed]
11. Kovacs, W.J.; Olivier, L.M.; Krisans, S.K. Central role of peroxisomes in isoprenoid biosynthesis. *Prog. Lipid Res.* **2002**, *41*, 369–391. [CrossRef] [PubMed]
12. Lange, B.M.; Croteau, R. Isopentenyl diphosphate biosynthesis via a mevalonate-independent pathway: Isopentenyl monophosphate kinase catalyzes the terminal enzymatic step. *Proc. Natl. Acad. Sci. USA* **1999**, *96*, 13714–13719. [CrossRef] [PubMed]
13. Lange, B.M.; Wildung, M.R.; McCaskill, D.; Croteau, R. A family of transketolases that directs isoprenoid biosynthesis via a mevalonate-independent pathway. *Proc. Natl. Acad. Sci. USA* **1998**, *95*, 2100–2104. [CrossRef]
14. Lichtenthaler, H.K. The 1-deoxy-D-xylulose-5-phosphate pathway of isoprenoid biosynthesis in plants. *Annu. Rev. Plant Biol.* **1999**, *50*, 47–65. [CrossRef] [PubMed]
15. Kuzuyama, T.; Takagi, M.; Kaneda, K.; Watanabe, H.; Dairi, T.; Seto, H. Studies on the nonmevalonate pathway: Conversion of 4-(cytidine 5′-diphospho)-2-C-methyl-D-erythritol to its 2-phospho derivative by 4-(cytidine 5′-diphospho)-2-C-methyl-D-erythritol kinase. *Tetrahedron Lett.* **2000**, *41*, 2925–2928. [CrossRef]
16. Lüttgen, H.; Rohdich, F.; Herz, S.; Wungsintaweekul, J.; Hecht, S.; Schuhr, C.A.; Eisenreich, W. Biosynthesis of terpenoids: YchB protein of Escherichia coli phosphorylates the 2-hydroxy group of 4-diphosphocytidyl-2C-methyl-D-erythritol. *Proc. Natl. Acad. Sci. USA* **2000**, *97*, 1062–1067. [CrossRef] [PubMed]
17. Ahn, C.S.; Pai, H.S. Physiological function of *IspE*, a plastid MEP pathway gene for isoprenoid biosynthesis, in organelle biogenesis and cell morphogenesis in *Nicotiana benthamiana*. *Plant Mol. Biol.* **2008**, *66*, 503–517. [CrossRef] [PubMed]
18. Kim, S.M.; Kim, Y.B.; Kuzuyama, T.; Kim, S.U. Two copies of 4-(cytidine 5′-diphospho)-2-C-methyl-d-erythritol kinase (CMK) gene in *Ginkgo biloba*: Molecular cloning and functional characterization. *Planta* **2008**, *228*, 941–950. [CrossRef] [PubMed]
19. Ji, K.S.; Wang, P.P.; Wang, J.L. Research progress on in vitro culture of pine tree species. *J. Nanjing For. Univ. Nat. Sci. Ed.* **2015**, *39*, 142–148.
20. Ran, J. Transcriptome analysis of needle and root of *Pinus massoniana* in response to continuous drought stress. *Plants* **2021**, *10*, 769. [CrossRef] [PubMed]
21. Zhu, P.H.; Chen, S.; Ji, K.S. Research progress on terpenoid synthase and its gene family in *Pinaceae*. *J. Nanjing For. Univ. Nat. Sci. Ed.* **2021**, *45*, 233–244.
22. Yang, Z.Q. Research progress and breeding strategies on genetic improvement of high-yield resin in *Pinus massoniana*. *Guangxi For. Sci.* **2015**, *44*, 317–324.
23. Banerjee, A.; Sharkey, T.D. Methylerythritol 4-phosphate (MEP) pathway metabolic regulation. *Nat. Prod. Rep.* **2014**, *31*, 1043–1055. [CrossRef]
24. Heidari Japelaghi, R.; Haddad, R.; Valizadeh, M.; Dorani Uliaie, E.; Jalali Javaran, M. High-efficiency agrobacterium-mediated transformation of tobacco (*Nicotiana tabacum*). *J. Plant Mol. Breed.* **2018**, *6*, 38–50.
25. Gershenzon, J.; Dudareva, N. The function of terpene natural products in the natural world. *Nat. Chem. Biol.* **2007**, *3*, 408–414. [CrossRef] [PubMed]
26. Bork, P.; Sander, C.; Valencia, A. Convergent evolution of similar enzymatic function on different protein folds: The hexokinase, ribokinase, and galactokinase families of sugar kinases. *Protein Sci.* **1993**, *2*, 31–40. [CrossRef] [PubMed]
27. Xiao, W.; Chang, H.; Zhou, P.; Yuan, C.; Zhang, C.; Yao, R.; Guo, X. Genome-wide identification, classification and expression analysis of GHMP genes family in *Arabidopsis thaliana*. *Plant Syst. Evol.* **2015**, *301*, 2125–2140. [CrossRef]

28. Zhu, P.; Chen, Y.; Wu, F.; Meng, M.; Ji, K. Expression and promoter analysis of MEP pathway enzyme-encoding genes in *Pinus massoniana* Lamb. *PeerJ* **2022**, *10*, e13266. [CrossRef] [PubMed]
29. Chen, X.M.; Chen, B.W.; Li, K.P. Correlation analysis between *GGPPS* gene and resin production capacity in *Pinus massoniana*. *Mol. Plant Breed.* **2018**, *16*, 5247–5254.
30. Mangas, S.; Bonfill, M.; Osuna, L.; Moyano, E.; Tortoriello, J.; Cusido, R.M.; Palazón, J. The effect of methyl jasmonate on triterpene and sterol metabolisms of *Centella asiatica*, *Ruscus aculeatus* and *Galphimia glauca* cultured plants. *Phytochemistry* **2006**, *67*, 2041–2049. [CrossRef] [PubMed]
31. van Schie, C.C.N.; Haring, M.A.; Schuurink, R.C. Tomato linalool synthase is induced in trichomes by jasmonic acid. *Plant Mol. Biol.* **2007**, *64*, 251–263. [CrossRef] [PubMed]
32. Keeling, C.I.; Bohlmann, J. Diterpene resin acids in conifers. *Phytochemistry* **2006**, *67*, 2415–2423. [CrossRef] [PubMed]
33. Martin, D.; Tholl, D.; Gershenzon, J.; Bohlmann, J. Methyl jasmonate induces traumatic resin ducts, terpenoid resin biosynthesis, and terpenoid accumulation in developing xylem of Norway spruce stems. *Plant Physiol.* **2002**, *129*, 1003–1018. [CrossRef]
34. Wang, W.; Wang, M.Y.; Zeng, Y.; Chen, X.; Wang, X.; Barrington, A.M.; Nieuwenhuizen, N.J. The terpene synthase (TPS) gene family in kiwifruit shows high functional redundancy and a subset of TPS likely fulfil overlapping functions in fruit flavour, floral bouquet and defence. *Mol. Hortic.* **2023**, *3*, 9. [CrossRef]
35. Estévez, J.M.; Cantero, A.; Reindl, A.; Reichler, S.; León, P. 1-Deoxy-D-xylulose-5-phosphate synthase, a limiting enzyme for plastidic isoprenoid biosynthesis in plants. *J. Biol. Chem.* **2001**, *276*, 22901–22909. [CrossRef]
36. Takahashi, S.; Kuzuyama, T.; Watanabe, H.; Seto, H. A 1-deoxy-D-xylulose 5-phosphate reductoisomerase catalyzing the formation of 2-C-methyl-D-erythritol 4-phosphate in an alternative nonmevalonate pathway for terpenoid biosynthesis. *Proc. Natl. Acad. Sci. USA* **1998**, *95*, 9879–9884. [CrossRef] [PubMed]
37. Yuan, Y.; Ren, S.; Liu, X.; Su, L.; Wu, Y.; Zhang, W.; Zhang, Y. SlWRKY35 positively regulates carotenoid biosynthesis by activating the MEP pathway in tomato fruit. *New Phytol.* **2022**, *234*, 164–178. [CrossRef]

Disclaimer/Publisher's Note: The statements, opinions and data contained in all publications are solely those of the individual author(s) and contributor(s) and not of MDPI and/or the editor(s). MDPI and/or the editor(s) disclaim responsibility for any injury to people or property resulting from any ideas, methods, instructions or products referred to in the content.